RESEARCH ARTICLE

Proteome network analysis of skeletal muscle in lignan-enriched nutmeg extract-fed aged mice

Je-Ho Lee[1†], Hyuno Kang[2†], Gyung-Tae Ban[1†], Beom Kyu Kim[1†], JaeHyeon Lee[3†], Heeyoun Hwang[4], Hwa-Seung Yoo[5], Kun Cho[6*] and Jong-Soon Choi[2,7*]

Abstract

Sarcopenia, characterized by reduced muscle mass and fiber number leading to muscular atrophy, has been asso-ciated with serious socioeconomic challenges among the elderly in developed countries. Therefore, preventing sarcopenia could be a promising strategy for achieving a healthy aging society. Nutmeg (*Myristica fragrans*) has been used as a spice to increase flavor and prevent putrefaction of food. Nutmeg contains various bioactive components that improve muscle activity. To determine the potential effect of lignan-enriched nutmeg extract (LNX) on sarco-penia, LNX (100 mg/kg body weight)-fed aged mice were subjected to forced exercise. Herein, aged (22-month-old) mice fed LNX for three weeks exhibited a shortened and thickened soleus muscle. The ratio of the soleus muscle mass (%) to body weight was significantly increased in LNX-fed aged mice. The relative increase in muscle mass in LNX-fed aged mice improved exercise activities, including rotarod, swimming, and grip strength test results. Proteome profiles of the soleus muscle of LNX-fed mice were used to analyze protein–protein interaction network. Several myosin heavy chain isoforms were found to interact with actin, ACTA1, which functions as a hub protein. Furthermore, the expres-sion of myogenic proteins, such as MYH1, MYH4, and ACTA1, was dose-dependently increased in vivo. In result, our functional proteomic analysis revealed that feeding LNX restored muscle proteins in aged mice.

Keywords Nutmeg, Sarcopenia, Exercise activity, Protein–protein interaction network

†Je-Ho Lee, Hyuno Kang, Gyung-Tae Ban, Beom Kyu Kim and JaeHyeon Lee equally contributed in this study

*Correspondence:
Kun Cho
chokun@kbsi.re.kr
Jong-Soon Choi
jschoi@kbsi.re.kr
[1] Geron Biotech Ltd., Daejeon 34133, Republic of Korea
[2] Division of Analytical Science, Korea Basic Science Institute, Daejeon 34133, Republic of Korea
[3] Department of Cancer Preventive Material Development, College of Korean Medicine, Kyung Hee University, Seoul 02447, Republic of Korea
[4] Research Center for Bioconvergence Analysis, Korea Basic Science Institute, Cheongju 28119, Republic of Korea
[5] East-West Cancer Center, Seoul Korean Medicine Hospital of Daejeon University, Seoul 05836, Republic of Korea
[6] Center for Research Equipment, Korea Basic Science Institute, Cheongju 28119, Republic of Korea
[7] Graduate School of Analytical Science and Technology, Chungnam National University, Daejeon 34134, Republic of Korea

Lee *et al. Journal of Analytical Science and Technology*   (2023) 14:11

Page 2 of 10

Introduction

Skeletal muscle is the largest organ by mass in the human body, in which muscle status indicates health and longevity of an individual. It reveals various physiological symptoms as it ages, including deterioration of functions, such as movement, respiration, vision, body temperature control, and metabolic homeostasis. Human muscle mass peaks during 30s, subsequently decreasing by approximately 1% annually, and falling sharply in 70s (Kalyani et al. 2014). This loss of muscle mass, called sarcopenia, can result in early death and reduce the quality of life, ultimately leading to fall-related fractures and increased mortality rates (Xie et al. 2021). Currently, there is no therapeutic agent available to prevent sarcopenia. Consumption of adequate proteins, vitamin D and strength training have been recommended to minimize muscle loss (Uchitomi et al. 2020). Long-term use of creatine supplements, known as muscle boosters, can cause liver and kidney damage among the elderly. Additionally, whey protein concentrate, often used as a protein supplement, contains lactose, which can cause digestive problems in this population (Souza et al. 2009). Pharmacological strategies for muscle development include the use of growth and sex hormones, insulin-like factors and myostatin inhibitors. Bimagrumab (Novartis), RG6206 (Roche) and ACE-031 (Acceleron) have been developed and examined to prevent muscular dystrophy; however, long-term use of these drugs could induce renal toxicity (Rooks et al. 2017; Dao et al. 2020; Campbell et al. 2017).

Several studies have explored natural products having potentials in improving muscle performance. For example, natural herbal plants from tropical regions like Indonesia reportedly exhibit potential health benefits. In addition, some herbal plants are rich in bioactive ingredients, such as catechins, resveratrol and curcumin, known to contribute to skeletal muscle development (Pratiwi et al. 2018). In particular, nutmeg is known to exhibit potential effects on various age-related diseases (Lestari et al. 2012). Nutmeg (*Myristica fragrans*), mostly cultivated in India, South Africa and Indonesia, has been used as a flavoring agent in foods and as an oriental medicine for diarrhea, abdominal distension, vomiting and appetite loss. Nutmeg extract contains bioactive lignan compounds, such as nectandrin B, fragransin A and tetrahydrofuroguaiacin B (Jang et al. 2019), which are beneficial for treating obesity, type 2 diabetes and other metabolic disorders (Hien et al. 2011). In animal models, nectandrin B was shown to prevent adult diseases by activating the AMPK pathway (Nguyen et al. 2010). Despite known medicinal benefits, excessive ingesting of nutmeg can induce toxic side effects, leading to delirium. Alkylbenzene derivatives, such as myristicin, elemicin

and safrole, are responsible for such toxicity (Du et al. 2014). Among these, myristicin is the most abundant toxic substance in nutmeg (Maeda et al. 2008). Reportedly, the methanol extract of nutmeg contains an average of 2.1% myristicin (Hallström and Thuvander 1997). One of the key aspects in preparation of nutmeg to consume is minimizing myristicin concentration below nontoxic level and maximizing beneficial ingredients such as nectandrin B.

In the present study, we aimed to investigate whether exercise performance was enhanced in aged mice fed a lignan-enriched nutmeg extract (LNX). We have established the optimal conditions for preparing LNX, which would comprise minimal levels of toxic myristicin (less than 0.5%) and maximum nectandrin B, an active ingredient (Jang et al. 2019). After oral administration of LNX for three weeks in C57BL/6 mice, the hindlimb muscles were dissected to estimate the anatomical indices. Exercise performance was evaluated as previously described (Xie et al. 2021). Rotarod, wire-hanging, swimming and grip strength tests were performed to evaluate muscle activity in young and aged control, and LNX-fed aged mice. Muscle proteomes of LNX-fed aged mice were cataloged, and a protein network was constructed from the soleus muscle using a well-established shotgun proteomic method (Jang et al. 2020). We found that myosin heavy chain isoforms in muscles were increased in LNX-fed aged mice, and their expression levels were verified by immunoblotting analysis. The findings of the present study provide further insights into the potential of lignan compounds as therapeutic agents to overcome sarcopenia.

Materials and methods

Animal treatment

Herein, we used C57BL/6 male mice supplied by the Animal Facility of Aging Science at Gwangju Center in the Korea Basic Science Institute (KBSI). All animals (3- and 22-month-old mice) were maintained at 22 ± 2 °C, $55 \pm 15\%$ humidity, and a 12 h light/12 h dark cycle. The experimental group was divided into four groups: young control (3-month-old), aged control (22-month-old), and 10 and 100 mg/kg body weight (mpk) LNX-fed aged mice groups. LNX was orally administered once daily for three weeks. Animal experiments were approved and followed the regulations of the KBSI Institutional Animal Care and Use Committee (KBSI-20–30 and KBSI-IACUC-21–28).

Measurement of muscle mass

The body weights of C57BL/6 mice were measured daily before LNX administration. Upon completion of exercise paradigms, all mice were anesthetized using isoflurane

Lee *et al. Journal of Analytical Science and Technology*   (2023) 14:11

Page 3 of 10

and then sacrificed by exsanguination, cutting the posterior vena cava and abdominal aorta. After skinned and photographed hindlimbs, the soleus and the gastrocnemius muscles were independently dissected, and the length and the width were measured using a caliper. Each muscle was weighed using an electronic scale (HR-250AZ; Coretech, Hwasung, Korea).

Histological observation of skeletal muscle

The gastrocnemius and the tibialis anterior muscles of hindlimbs were independently separated and fixed in 4% paraformaldehyde for 48 h. After dehydration and paraffin embedding, 5-μm-thick cross-sections were prepared using a microtome (Microm STP 120, Thermo Fischer Scientific, Waltham, MA). Serial sections were stained with hematoxylin and eosin using Vitroview™ Masson's trichrome staining. Images of muscle fibers were obtained using a microscope (Nikon Eclipse Ti, Tokyo, Japan) with a camera (Nikon DS-Ri2, Tokyo, Japan) operated by NIS-Elements BR software.

Physical exercise performance

The rotarod test was conducted using the Rotarod instrument (SB Technology, Miami, FL), as described previously (Vaught et al. 1985). The rotarod measurements were performed in fixed and accelerating modes, rotating at 4 rpm and 4–40 rpm, respectively. Mice were acclimatized for 1 h before testing, and re-training was performed for 1 min in fixed mode. The main experiment was performed in the accelerating mode, and the time taken to fall off the rotarod was recorded.

In the wire-hanging test, mice were hung on a horizontal bar, approximately 50 cm above the ground. The strength of the forelimb was determined by measuring the duration and latency before falling from the bar. The test was repeated after intervals of at least 1 min.

The swimming test was performed as previously described (Nunez 2008). Briefly, mice were placed on a platform (touchable by their feet) at one end of a 120 cm round water tank, which was sufficiently wide to prevent limbs from touching the walls. Non-fat dry milk was added to the tank water to ensure the tank bottom was not visible. The test mice were allowed to swim with their backs to the platform using different starting directions. An animal behavior tracking system recorded the movement route to calculate the swimming speed.

The grip strength test was performed using a digital force gauge (Ametek, Berwyn, PA), as previously described (Seto et al. 2011). The equipment comprised a wire (1 mm in diameter) installed 35 cm high. The mouse was allowed to grip the wire using only the forelimbs, and the force at which the wire was released on pulling the tail was recorded using the Chatillon Digital Force Gauge PC program.

Protein sample preparation

The mouse soleus muscle was selected as the protein source for proteomic analysis. Using a surgical scalpel, the muscle tissue was cut into 5 mm × 5 mm × 5 mm pieces, placed in an Eppendorf tube, and washed three times for 10 min with 50 ml of saline containing a protease inhibitor (Protease Inhibition Cocktail Tablet, Roche). Muscle tissue (100 mg) was homogenized in 1 ml of mammalian protein extraction buffer (GE Healthcare, Chicago, IL). The protein concentration was quantified using a BCA assay kit (Thermo Fischer, Seoul, Korea). For proteomic analysis, in-solution trypsin digestion was performed as described previously (Lee et al. 2015). Trypsin proteolysis was performed by reduction with dithiothreitol and alkylation with indoleacetic acid. Trypsin digestion was performed at 37 °C for 16 h, followed by lyophilization prior to mass spectrometry (MS).

Mass spectrometry analysis

MS analysis was performed as previously described (Michalski et al. 2011). Dried peptides were reconstituted in 0.02% formic acid and 0.5% acetic acid to a final concentration of 100 ng/μl. Peptide sample (10 μL) was eluted using a nanoACQUITY UPLC 2G-V/V Trap 5 μm Symmetry C_{18} (180 μm × 20 mm) trapping column (Waters, Ireland) with 10 μL/min for 10 min, with the flow rate maintained at 120 nL/min. The specification of analytical column is 3 μm C_{18} AQ (100 μm × 15 cm) (NanoLC, Thermo Scientific, Waltham, MA). The peptides were eluted with a gradient of 0–65% acetonitrile for 80 min. All MS and tandem MS spectra were detected using a Q-Exactive Mass Spectrometer (Thermo Fischer Scientific, Waltham, MA) in a data-dependent manner. Each full MS was scanned in the range of 300–2000 *m/z*, and the most abundant precursor ion peaks were obtained from MS spectra. All MS/MS spectra were acquired in a data-dependent mode for fragmentation of the 5 most abundant peaks from the full MS scan with 35% normalized collision energy. The separated peptide ions eluted from the analytical column were entered into the mass spectrometer at an electrospray voltage of 2.2 kV. The dynamic exclusion duration was set at 180 s and exclusion mass width 0.5 Da. MS spectra were acquired with a mass range of 150–2000 *m/z*.

Protein identification and quantification

Raw MS data were analyzed using the MaxQuant software (ver. 1.5.3.17, www.maxquant.org), as described

previously (Cox and Mann 2008). The MS/MS spectra were identified as proteins using forward and reverse sequences from the UniProt mouse database (http://www.uniprot.org; released in 2018_10, 59,345 entries) in the Andromeda search engine (integrated with Max-Quant). The precursor and fragment masses were matched at initial mass tolerance levels of 6 and 20 ppm, respectively. Two miscleavages were allowed, and Cys-carbamidomethylation $(+57)$ and Met-oxidation $(+16)$ were considered fixed and variable protein modifications, respectively. Protein quantification of the liquid chromatography with tandem MS (LC–MS/MS) spectra was analyzed using a semi-quantitative method with Max-Quant ion scoring. Qualified scoring peptides were considered to satisfy the threshold set above $p < 0.05$, peptide level ≤ 0.05, and false discovery rate < 0.05 in the decoy database. Peptides were identified with monoisotopic mass selected, a precursor mass tolerance of 25 ppm, and a fragment mass tolerance of 25 ppm, two missed trypsin cleavage and fixed modification of carbamidomethyl cysteine. Threshold score/expectation value for accepting individual spectra was based on Mascot ion score threshold (0.05) as the standard ion score threshold specifically calculated by Mascot for each database search.

Bioinformatics analysis

Gene Ontology (GO) was analyzed with qualified protein data using InterPro2Go mapping (www.ebi.ac.kr/GOA/InterPro2GO). GO annotation used search parameters in InterProScan. The top-ten BLAST hits were arranged by listing those with an E-value of $\leq 1 \times 10^{-3}$ for each query sequence. Statistical significance was determined using an individual *t*-test module from the scipy.stats module (scipy.org), with an in-house program coded by Python 3.8, where significant proteins were selected by $p < 0.05$ and fold-change > 1.5. Protein–protein interaction (PPI) network was constructed using the Search Tool for the Retrieval of INteracting Genes/proteins (STRING) database (string-db.org), maximizing the networks as a default setting.

Immunoblot analysis

Soleus muscle proteins were extracted with extraction buffer [50 mM Tris–HCl (pH 7.4), 2 mM EDTA, 100 μg/ml leupeptin, 20 μg/ml aprotinin, and 100 mM NaCl]. Protein samples (40 μg) were subjected to 10% sodium dodecyl sulfate–polyacrylamide gel electrophoresis (SDS-PAGE), and the gel was transferred to a polyvinylidene difluoride (PVDF) membrane. The membrane was blocked for 1 h with 5% skimmed milk in TTBS containing 50 mM Tris–HCl (pH 8.2), 0.1% Tween 20, and 150 mM NaCl. Subsequently, the blots were incubated overnight at 4 °C with primary antibodies (Santa Cruz Biotechnology, Dallas, TX) against Titin, Myh1, Myh4, and Acta1. The blot was washed five times for 5 min with TTBS and incubated with horseradish peroxidase (HRP)-conjugated goat anti-mouse IgG (1:5000) secondary antibody. Signals were detected using enhanced chemiluminescence (MilliporeSigma, Burlington, MA) and visualized using a Chemi-Doc™ Imaging System (Bio-Rad, Hercules, CA). The relative expression of the target protein was normalized to that of β-actin, an endogenous housekeeping protein.

Statistical analysis

Experimental animal data were analyzed using the Mann–Whitney U test. Comparisons were statistically significant at a 95% confidence level. One-way analysis of variance (ANOVA) was used to compare multiple groups. Data analyses were performed using GraphPad Prism 5.0 (GraphPad Software). Statistical evaluation of the proteome network analysis was performed using Student's *t*-test, and $p \leq 0.05$ were deemed statistically significant.

Results and discussion

In the present study, we evaluated the exercise performance of LNX-fed aged mice and further performed a proteomic network analysis of skeletal muscle to identify core proteins involved in muscular enhancement. LNX, the test substance, was obtained by two-step ethanol extraction, as previously reported (Nguyen et al. 2010). We concentrated nectandrin B, an active ingredient, by up to 6.1% after the second extraction with 80% ethanol, whereas the content of myristicin, the toxic compound, was only 0.04% (data not shown). Isolation and enrichment of LNX by ethanol-extraction resulted in the following yield of principle lignans: nectandrin B (41.66 mg/g), fragransin A2 (0.18 mg/g), and verrucosin (2.32 mg/g) (Additional file 1: Fig. S1). The final dried extracts of LNX were subjected to subsequent animal experiments and proteomic analysis.

After feeding naturally aged C57BL/6 mice with LNX for three weeks, the debilitated fore- and hindlimb muscles were improved (Additional file 1: Fig. S2A). Microscopic observation of hindlimb muscles (gastrocnemius and tibialis anterior) revealed that the diameters of hindlimb muscle fibers in aged mice were smaller than those in young mice. In addition, myofibers of tibialis anterior muscle in aged mice were more loosely arranged than young mice. However, skeletal muscles of LNX (100 mpk)-fed aged mice showed marked recovery to the level of young mice in terms of myofiber diameter and muscle fiber compactness (Additional file 1: Fig. S2B).

Testosterone, myostatin inhibition, and exercise are known to increase contractile proteins (actin and myosin) in muscle fibers via anabolic intervention, resulting in hypertrophy (Verdijk et al. 2009). Conversely, an age-related decrease in muscle mass and strength are typical features of sarcopenia.

Skeletal muscles of LNX-fed aged mice were characterized by gain of body weight and muscle indices. The anatomical indices included width, length and mass per body weight of the calf muscles. The gastrocnemius and the soleus muscles in hindlimbs were dissected, and anatomical indices were measured. Although low-dose LNX-fed mice showed slight weight loss when compared with untreated controls, this tendency was not observed in high-dose LNX-fed old mice. Thus, the effect of LNX on body weight gain was not correlated between LNX-treated and untreated groups, regardless of age (Fig. 1A). However, the morphology of skeletal muscles revealed a clear relationship with the LNX feeding dose. In LNX-fed aged mice, the lengths of gastrocnemius and soleus muscles were decreased, whereas the widths of both muscles were increased in a dose-dependent manner (Fig. 1B, C). LNX feeding specifically affected both anatomical indices of the soleus muscle. In high-dose LNX-fed aged mice, the soleus muscle mass to body weight ratio was significantly increased ($p < 0.05$; Fig. 1D). This finding is comparable with that of a previous report, demonstrating that *Schisandrae fructus* can enhance both gastrocnemius and splenic muscles in aged mice (Kim et al. 2018), whereas LNX specifically increased the ratio of the soleus muscle mass to body weight. Likewise, it has been reported that continuous feeding of C57BL/6 mice with a natural product, 2,6-dimethoxy-1,4-benzoquinone, for 7 weeks can increase muscle mass and strength (Yoo et al. 2021).

Several studies have reported the potential of phytochemicals to suppress or recover from progressive sarcopenia, affording a sarcopenia recovery program. *Schizandra chinensis* exhibits an inhibitory effect on muscle fiber in mice and suppresses muscular dystrophy by increasing protein synthesis in human myocytes (Choi 2017; Kim et al. 2016). Recently, nutmeg extract was found to increase skeletal muscle weight in aged rats, mainly via IGF1-Akt-mTOR signaling and autophagy inhibition (Pratiwi et al. 2018). Therefore, we evaluated the effect of LNX on exercise performance in C57BL/6 mice. Examination of several indices confirmed in vivo efficacy of LNX in terms of exercise performance using rotarod, wire-hanging, swimming and grip strength tests. In the rotarod test, endurance time in the accelerating mode (4 to 40 rpm) was increased in both LNX-treated aged groups; in particular, LNX feeding showed a significant increase specifically in aged mice ($p < 0.05$; Fig. 2A).
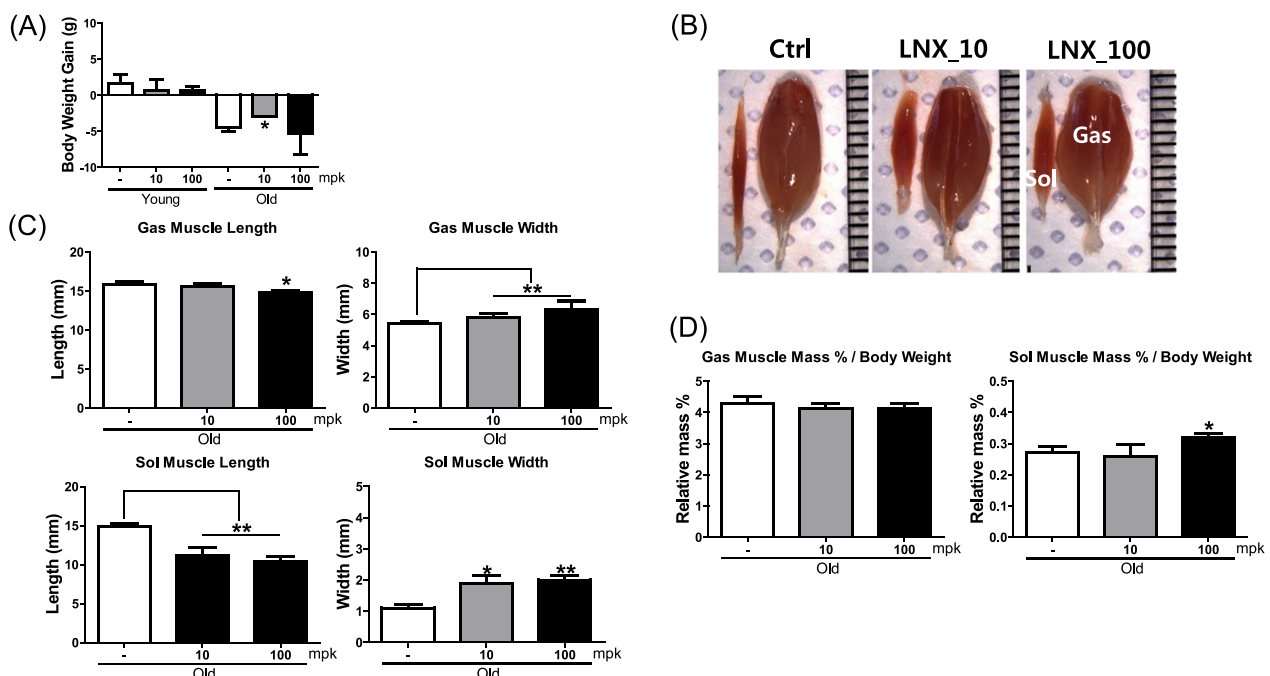
Fig. 1 Phenotypical and anatomical changes of LNX-fed mice. **A** Body weight gain. **B** Images of dissected gastrocnemius (Gas) and soleus (Sol) muscles. Each gradation on a rule is 1 mm scale. **C** Dimensions of dissected Gas and Sol muscles. **D** Weight of each Gas and Sol muscle divided by body weight. Data represent the mean ± standard deviation of triple or quadruple experiments. Statistical significance * $p < 0.05$, ** $p < 0.01$
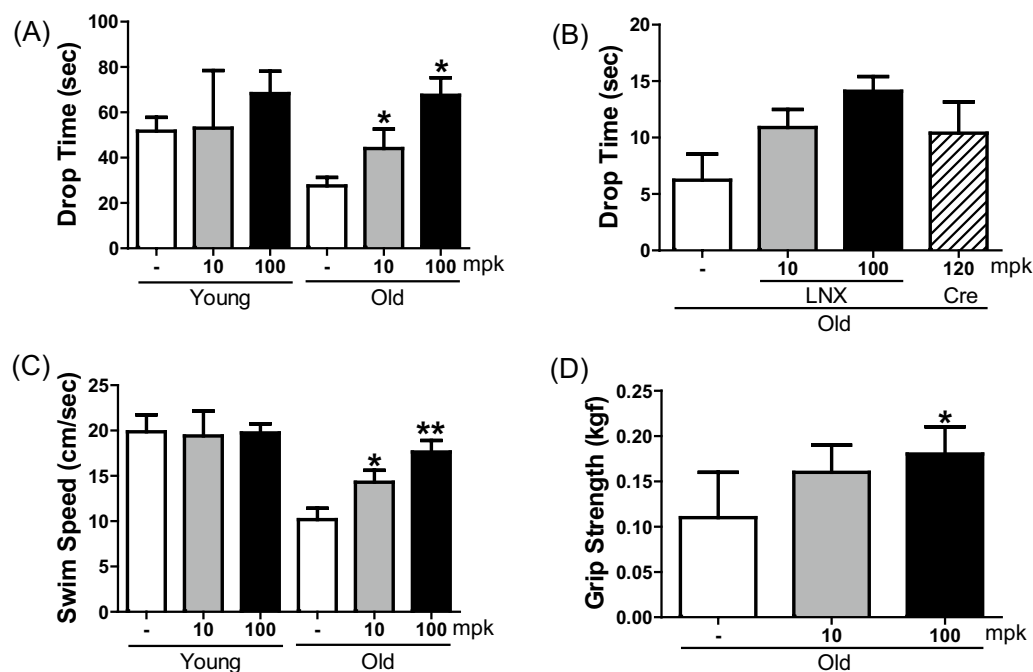
Fig. 2 Improved effects of LNX on exercise activities in LNX-fed mice. **A** Rota-rod, **B** wire-hanging, **C** swimming, and **D** grip strength tests were performed in LNX-fed mice. Data represent mean ± standard deviation of triple or quadruple experiments. Statistical significance * $p < 0.05$, ** $p < 0.01$

The wire-hanging test revealed an increasing pattern of endurance time in LNX-fed aged mice with no statistical significance (Fig. 2B). Creatine, known as a muscle booster, can increase wire-hanging endurance time, similar to LNX. However, administration of 120 mpk creatine for three weeks caused severe cirrhosis, while the livers of LNX-fed old mice appeared normal (Additional file 1: Fig. 3). Creatine is used as an energy source by phosphocreatine kinase in muscles; however, excessive creatine use in the elderly may burden the liver and kidney (Poortmans and Francaux 2000).

Considering the swimming test, no difference was detected in young mice fed in the presence and absence of LNX (Fig. 2C). However, swimming speed of aged mice was approximately 50% less than that of young mice. Interestingly, swimming speed was recovered by up to 89% of the young control in 100 mpk LNX-fed aged mice. In particular, low- and high-dose LNX-fed aged mice showed statistical significance at $p < 0.05$ and $p < 0.01$, respectively. The forelimb grip strength was measured in aged mice fed 10 or 100 mpk LNX. Grip strength was significantly increased in 100 mpk LNX-fed aged mice ($P < 0.05$; Fig. 2D). Collectively, these results suggest that nectandrin B, as the main lignan compound in LNX, enhanced exercise activity by increasing muscle myofibers. Previously, we reported that nectandrin

B could reduce intracellular reactive oxygen species levels in human fibroblasts and prevent senescence by activating AMPK signaling (Jang et al. 2019). In a rejuvenation program, concurrent application of anticancer drugs, dasatinib and quercetin, in mice as a senolytic cocktail therapy was shown to improve muscle strength, treadmill exercise ability, and enhance grip strength (Xu et al. 2018). Administering the senolytic drug ABT263 for 4 weeks could improve skeletal muscle (Chang et al. 2016), and aged mice fed ruxolitinib (INCB18424) for 10 weeks increases hanging duration and grip strength (Xu et al. 2015). Therefore, the senolytic potential of LNX needs to be explored.

To identify core proteins induced by LNX feeding, shotgun proteomic analysis was performed with the soleus muscle of mouse hindlimb. Shotgun proteomics was used with modifications, except for the MaxQuant database from a previous method (Lee et al. 2015). Considering the experimental design, five groups were classified as young (3-month-old) and aged (22-month-old) controls, and LNX (10, 30, 100 mpk)-fed aged mice. The distribution of protein abundance from 15 samples is shown using a box plot (Additional file 1: Fig. S4). The average values for all groups were constant at 18, and the degree of variance was similarly normalized, suggesting that the proteomic conditions were well established.

Table 1 Summary of quantitative proteome analysis. Data are presented in three groups: muscles of young, old, and LNX (100 mpk)-fed old mice

Group		Fold change	Number of proteins	Remarks
Old vs Young	$p* < 0.05$	$|FC| \geq 1.5$	35	Additional file 2: Table S1
		$-1.5 < FC < 1.5$	55	
	$p \geq 0.05$		96	
LNX-Old vs Old	$p* < 0.05$	$|FC| \geq 1.5$	16	Additional file 2: Table S2
		$-1.5 < FC < 1.5$	6	
	$p \geq 0.05$		13	

*p-value was calculated from three independent proteins altered in old mice compared to that in young mice or in LNX-fed old mice compared to that in old mice

The number of proteins indicated in this table was determined using general proteome search criterions

A total of 221 proteins were summarized according to the comparison group, statistical significance, and fold-change (Table 1). Among them, 35 proteins between aged and young mice groups showed a fold-change of ˃ 1.5, with statistical significance at $p < 0.05$ (Additional file 2: Table S1). Furthermore, 16 proteins were significantly altered between LNX (100 mpk)-fed and -unfed aged mice, with a fold-change of ˃1.5 (Additional file 2: Table S2). Heat map analysis revealed that 13 proteins were significantly recovered by LNX feeding in aged mice (Additional file 1: Fig. S5), including LNX-induced up- and down-regulated proteins in aged mice (Table 2). Interestingly, increased expression of heat shock 70 protein (Hspa1b) was consistent with that reported in muscular dystrophic mdx mice (Carberry et al. 2014). In addition, zinc finger proteins, Zfp882 and Zc3b13 were increased in senescent mouse muscle tissue, similar to

enhanced expression of zinc finger in muscle cells under muscular dystrophy conditions (Lynch et al. 2019). If these zinc finger proteins are marker proteins of aging, LNX could restore their expression to normal levels and afford clues regarding aging. Another interesting protein is LIM-binding protein, in which LIM and cysteine-rich domain 1 (LMCD1) regulate skeletal muscle hypertrophy (Ferreira et al. 2019). Likewise, in our proteomic analysis, the expression of LIM-binding protein 3 (Ldb3) was increased in aged mice; however, LNX administration decreased this expression, resulting in a young-like phenotype.

To address the biological function, proteins identified in the soleus muscles of aged mice and LNK (100 mpk)-fed aged mice were subjected to GO assessment via InterProScan. Based on the top priority of GO groups, components related to skeletal muscle were

Table 2 List of recovered muscle proteins in LNX-fed old mice from up- or down-regulated proteins of old versus young mice

| Acc. #	Protein name	Description	Mr (Da)	Fold change (O vs Y)	Fold change (LX-O vs O)
Proteins altered by LNX from down-regulated proteins in old mice					
Q99LX0	Park7	Protein/nucleic acid deglycase DJ-1	20,021	− 1.76	+ 1.58
P63038	Hspd1	60 kDa heat shock protein, mitochondria	61,055	− 1.58	+ 2.31
Proteins altered by LNX from up-regulated proteins in old mice					
E9PYJ9	Ldb3	LIM domain-binding protein 3	77,135	+ 1.77	− 5.61
D3Z7G7	Zfp882	Zinc finger protein 882 (fragment)	63,994	+ 2.80	− 3.33
Q8CGP6	Hist1h2ah	Histone H2A type 1-H	13,950	+ 2.04	− 2.93
E9Q784	Zc3h13	Zinc finger CCCH domain-containing protein13	203,755	+ 2.06	− 2.53
P17879	Hspa1b	Heat shock protein 70 kDa protein 1B	70,176	+ 1.69	− 2.23
Q6P6L5	Mybpc1	Myosin-binding protein C, slow-type	126,197	+ 1.51	− 2.12
Q6IFZ6	Krt77	Keratin, type II cytoskeletal 1b	61,359	+ 2.34	− 1.86
P29387	Gnb4	Guanine nucleotide-binding protein subunit β-4	37,379	+ 1.76	− 1.83
A2AT66	Ttn	Titin (fragment)	76,372	+ 1.56	− 1.76
F6RSJ3	Ttn	Titin (fragment)	130,483	+ 1.54	− 1.70
Q62000	Ogn	Mimecan	34,012	+ 1.85	− 1.64

assigned as the main GO groups (Additional file 2: Table S3). LNX-induced myofiber restoration was well matched with the GO analysis, in which myofibers consist of actin and myosin. This finding is consistent with that of a previous study, demonstrating that the expression of myosin, tropomyosin, and the small heat shock protein Hsp27 was reduced in aged mice (Carberry et al. 2012). Using the STRING database, a PPI network was constructed using whole soleus muscle proteomes from young, aged and LNK-fed aged mice (https://string-db.org). Several myosin heavy chain protein isoforms (Myh) were detected in the core cluster, with actin Acta1 as a hub protein (Fig. 3A). In addition, Ldb3 interacts with the surrounding actin proteins in the local network Group 3 (Fig. 3B). It can be speculated that Ldb3 regulates myosin and actin via PPI while acting antagonistically against LMCD1 as a positive regulator of muscle mass (Ferreira et al. 2019). Keratin 77 levels increased with age but were significantly decreased by LNX feeding. Krt77 interacts with Myh4, a component of the main protein network cluster.

When proteins were unpacked, it was confirmed that the actin isoforms, including muscle fiber proteins such as Group 1, form a network. Accordingly, immunoblotting confirmed the expression of Myh1 and Myh4 interacting with Acta1 in LNX-fed aged mouse muscles. The expressional changes in the soleus muscles of aged mice fed different LNX concentrations, centering on myogenic proteins, were verified by immunoblot analysis (Fig. 4). As shown in the heat map analysis (Additional file 1: Fig. 5), LNX slightly decreased Ttn expression; however, the expression levels of Myh1, Myh4, and Acta1 significantly increased in a dose-dependent manner. The expression of contractile proteins was in good agreement with the results of previous proteomic studies (Dowling et al. 2019). A muscle restoration study with a single compound, such as nectandrin B, verrucosin or fragransin A2, known components of LNX, could afford promising results for developing potent therapeutic drug candidates against sarcopenia.

Conclusions

Herein, we aimed to determine the effect of LNX, comprising the major lignan, nectandrin B, on exercise performance and examine the working mechanism using protein network analysis via shotgun proteomics. After a three-week treatment, LNX-fed aged mice showed increased soleus muscle mass to body weight ratio and enhanced exercise performance in rotarod, swimming and grip strength tests. Comparing rejuvenation-related proteins in LNX-fed aged mice, zinc finger protein, heat shock protein 70, and keratin were expressed, as reported in previous studies. Muscle protein network analysis revealed the muscle contraction protein Acta1 cluster and upregulation of Myh1, Myh4, and Acta1 confirmed by immunoblotting. In conclusion, LNX could be effective for aging-related sarcopenia, and bioactive lignans of LNX could be developed as potential therapeutic agents.
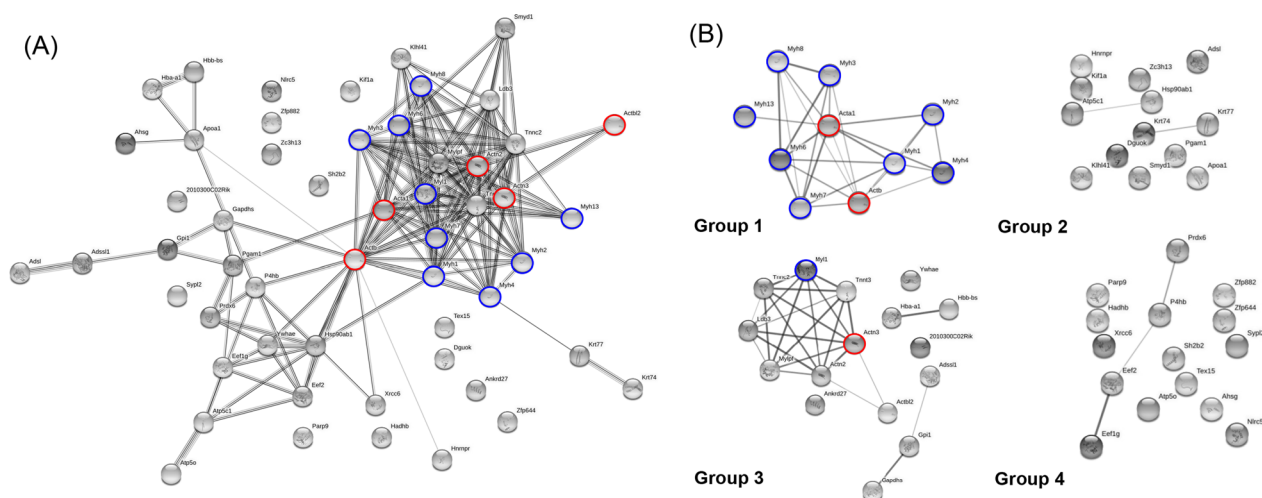
Fig. 3 Protein network analysis of whole mouse soleus muscle proteomes. Protein network was constructed using STRING database (https://string-db.org). **A** Full view of protein–protein interaction network. **B** Main protein–protein network (group 1) and satellite networks (group 2–4). Red and blue circle indicates actin and myosin isoforms, respectively

Lee *et al. Journal of Analytical Science and Technology*   (2023) 14:11

Page 9 of 10
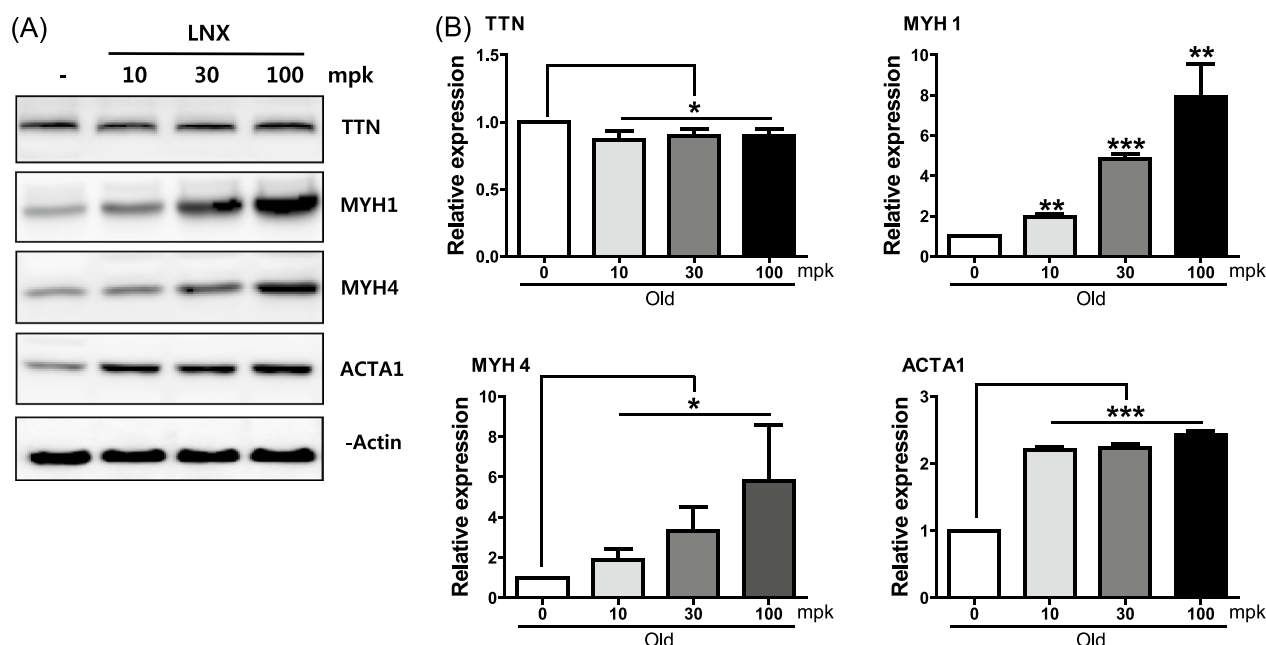
Fig. 4 Immunoblot analysis of soleus muscle proteins identified from LNX-fed old mice. **A** Gel images of immunoblotting. **B** Quantitative analysis of protein markers such as TTN, MYH1, MYH4, and ACTA1. Relative expression was presented as %control of old mice using the normalized levels of β-actin as internal control. *ns*, not significant, statistical significance at * $p < 0.05$, ** $p < 0.01$, *** $p < 0.001$

Supplementary Information

The online version contains supplementary material available at https://doi.org/10.1186/s40543-023-00377-2.

Additional file 1. **Figure 1** Isolation and enrichment of ethanol-extracted LNX. (A) UV chromatogram of ethanol-extracted LNX and yields of main lignan compounds from LNX. Mean±St Dev. Standard deviation was calculated by triplicate experiments. (B) Chemical structures of main lignan compounds from LNX. Analysis condition: equipment, Agilent 1200 series HPLC system; mobile phase, acetonitrile: 0.1% formic acid (4:6); stationary phase, Waters C18 column (5 μm pore size, 25 cm in length); detection wavelength, 234 nm; flow rate, 1.5 ml/min. **Figure 2** Dissection and microscopic images of skeletal muscles of LNX-fed mice. (A) Images of skeletal muscles. Left and right panel on each picture indicates fore and hind limb, respectively. Scale bar is 1 cm. (B) H&E staining of cross sections from gastrocnemius muscle and tibialis anterior. Abbreviations: mfb, microfibrils; mf, microfiber; pm, perimysium. Arrows indicate nuclei staining. Scale bar = 20 μm. **Figure 3** Anatomical changes of livers in (A) young, (B) LNX (100 mpk) and (C) creatine (120 mpk)-fed old mice. Scale bar = 1 cm. **Figure 4** Box plots of all proteome quantitates from four groups: young, old, LNX-fed old mice. Doses of LNX applied to old mice were 10, 30, and 100 mpk. Proteomic sample source was soleus muscle from each group. **Figure 5** Heat map analysis of mouse soleus muscle proteomes. Significantly altered 16 proteins in LNX-fed old vs. old mice soleus muscles. Red and blue color intensity means the degree of up- and down-regulation, respectively.

Additional file 2. **Table 1** List of significantly altered proteins in old mice muscle compared to young mice control. **Table 2** List of significantly altered proteins in LNX-fed old mice muscle compared to old mice control. **Table 3** List of GO-analyzed proteins identified commonly in old versus LNX (100 mpk)-fed old mice muscle. Top-ten ranked GO groups in number were listed according to (A) biological process, (B) molecular function, and (C) cellular function.

Availability of data and materials
The datasets used and/or analyzed during the current study are available from the corresponding author on reasonable request.

Declarations

Competing interests
The authors declare that they have no competing interests.

References

Campbell C, McMillan HJ, Mah JK, Tarnopolsky M, Selby K, McClure T, Wilson DM, Sherman ML, Escolar D, Attie KM. Myostatin inhibitor ACE-031 treatment of ambulatory boys with Duchenne muscular dystrophy: Results of a randomized, placebo-controlled clinical trial. Muscle Nerve. 2017;55:458–64.

Carberry S, Zweyer M, Swandulla D, Ohlendieck K. Profiling of age-related changes in the tibialis anterior muscle proteome of the mdx mouse model of dystrophinopathy. J Biomed Biotechnol. 2012;2012:691641.

Carberry S, Zweyer M, Swandulla D, Ohlendieck K. Comparative proteomic analysis of the contractile-protein-depleted fraction from normal versus dystrophic skeletal muscle. Anal Biochem. 2014;446:108–15.

Chang J, Wang Y, Shao L, Laberge RM, Demaria M, Campisi J, Janakiraman K, Sharpless NE, Ding S, Feng W, Luo Y, Wang X, Aykin-Burns N, Krager K, Ponnappan U, Hauer-Jensen M, Meng A, Zhou D. Clearance of senescent cells by ABT263 rejuvenates aged hematopoietic stem cells in mice. Nat Med. 2016;22:78–83.

Choi YH. Effects of Schisandrae fructus supplementation on apoptosis and inflammatory response in gastrocnemius muscle of dexamethasone-induced muscle atrophy mice. Herbal Formular Sci. 2017;25:363–73.

Cox J, Mann M. MaxQuant enables high peptide identification rates, individualized p.p.b. -range mass accuracies and proteome-wide protein quantification. Nat Biotechnol. 2008;26:1367–72.

Dao T, Green AE, Kim YA, Bae SJ, Ha SJ, Gariani K, Lee MR, Menzies KJ, Ryu D. Sarcopenia and muscle agingL a brief overview. Endocrinol Metab. 2020;35:716–32.

Dowling P, Zweyer M, Swandulla D, Ohlendieck K. Characterization of contractile proteins from skeletal muscle using gel-based top-down proteomics. Proteome. 2019;7:25.

Du SS, Yang K, Wang CF, You CX, Geng ZF, Guo SS, Deng ZW, Liu ZL. Chemical constituents and activities of the essential oil from Myristica fragrans against cigarette beetle Lasioderma serricorne. Chem Biodivers. 2014;11:1449–56.

Ferreira DMS, Cheng AJ, Agudelo LZ, Cervenka I, Chaillou T, Correia JC, Palmertz MP, Izadi M, Hansson A, Martinez-Redondo V, Valente-Silva P, Pettersson-Klein AT, Estall JL, Robinson MM, Nair KS, Lanner JT, Ruas JL. LIM and cysteine-rich domain1 (LMCD1) regulates skeletal muscle hypertrophy, calcium handling, and force. Skelet Muscle. 2019;9:26.

Hallström H, Thuvander A. Toxicological evaluation of myristicin. Nat Toxins. 1997;5:186–92.

Hien TT, Oh WK, Nguyen PH, Oh SJ, Lee MY, Kang KW. Nectandrin B activates endothelial nitric-oxide synthase phosphorylation in endothelial cells: role of the AMP-activated protein kinase/estrogen receptor α/phosphatidylinositol 3-kinase/Akt pathway. Mol Pharmacol. 2011;80:1166–78.

Jang HJ, Yang KE, Oh WK, Lee SI, Hwang IH, Ban KT, Yoo HS, Choi JS, Yeo EJ, Jang IS. Nectandrin B-mediated activation of the AMPK pathway prevents cellular senescence in human diploid fibroblasts by reducing intracellular ROS levels. Aging. 2019;11:3731–49.

Jang IS, Jo E, Park SJ, Baek SJ, Hwang IH, Kang HM, Lee JH, Kwon J, Son J, Kwon HJ, Choi JS. Proteomic analyses reveal that ginsenoside Rg3(S) partially reverses cellular senescence in human dermal fibroblasts by inducing peroxiredoxin. J Ginseng Res. 2020;44:50–7.

Kalyani RR, Corriere M, Ferrucci L. Age-related and disease-related muscle loss: the effect of diabetes, obesity, and other diseases. Lancet Diabetes Endocrinol. 2014;2:819–29.

Kim CH, Shin JH, Hwang SJ, Choi YH, Kim DS, Kim CM. Shisandrae fructus enhances myogenic differentiation and inhibits atrophy through protein synthesis in human myotubes. Int J Nanomed. 2016;11:2407–15.

Kim KY, Ku SK, Lee KW, Song CH, An WG. Muscle-protective effects of Schisandrae fructus extracts in old mice after chronic forced exercise. J Ethnopharmacol. 2018;212:175–87.

Lee DG, Nam J, Kim SW, Kang MY, An HJ, Kim CW, Choi JS. Proteomic analysis of reproduction proteins involved in litter size from porcine placenta. Biosci Biotechnol Biochem. 2015;79:1414–21.

Lestari K, Hwang JK, Kariadi SH, Wijaya A, Ahmad T, Subarnas A, Muchtaridi M. Screening for PPARγ agonist from *Myristica fragrans* Houtt seeds for the treatment of type 2 diabetes by in vitro and in vivo. Med Health Sci J. 2012;12:7–15.

Lynch SA, McLeod MA, Orsech HC, Cirelli AM, Weddell DS. Zinc finger protein 593 is upregulated during skeletal muscle atrophy and modulates muscle cell differentiation. Exp Cell Res. 2019;383:111563.

Maeda A, Tanimoto S, Abe T, Kazama S, Tanizawa H, Nomura M. Chemical constituents of Myristica fragrans Houttuyn seed and their physiological activities. Yakugaku Zasshi. 2008;128:129–33.

Michalski A, Cox J, Mamm M. More than 100,000 detectable peptide species elute in single shotgun proteomics runs but the majority is inaccessible to data-dependent LC-MS/MS. J Proteome Res. 2011;10:1785–93.

Nguyen PH, Le TVT, Kang HW, Chae J, Kim SK, Kwon K, Seo DB, Lee SJ, Oh WK. AMP-activated protein kinase (AMPK) activators from *Myristica fragrans* (nutmeg) and their anti-obesity effect. Bioorg Med Chem Lett. 2010;20:4128–31.

Nunez J. Morris water maze experiment. J vis Exp. 2008;19:897.

Poortmans JR, Francaux M. Adverse effects of creatine supplementation: fact or fiction? Sports Med. 2000;30:155–70.

Pratiwi YS, Lesmana R, Goenawan H, Sylviana N, Setiawan I, Tarawan VM, Lestari K, Abdulah R, Dwipa L, Purba A, Supratman U. Nutmeg extract increases skeletal muscle mass in aging rats partly via IGF1-AKT-mTOR pathway and inhibition of autophagy. Evid Based Complement Alternat Med. 2018;2018:2810840.

Rooks D, Praestgaard J, Hariry S, Laurent D, Petricoul O, Perry RG, Lach-Trifilieff E, Roubenoff R. Treatment of sarcopenia with Bimagrumab: results from a phase II, randomized, controlled, proof-of-concept study. J Am Geriatr Soc. 2017;65:1988–95.

Seto JT, Chan S, Turner N, MacArthur DG, Raftery JM, Berman YD, Quinlan KGR, Cooney GJ, Head SH, Yang N, North KN. The effect of α-actinin-3 deficiency on muscle aging. Exp Gerontol. 2011;46:292–302.

Souza RA, Miranda H, Xavier M, Lazo-Osorio RA, Gouvea HA, Cogo JC, Vieira RP, Ribeiro W. Effects of high-dose creatine supplementation on kidney and liver responses in sedentary and exercised rats. J Sports Sci Med. 2009;8:672–81.

Uchitomi R, Oyabu M, Kamei Y. Vitamin D and sarcopenia: potential of vitamin D supplementation in sarcopenia prevention and treatment. Nutrients. 2020;12:3189.

Vaught J, Pelley K, Costa LG, Sether P, Enna SJ. A comparison of the antinociceptive responses to GABA-receptor against THIP and baclofen. Neuropharmacol. 1985;24:211–6.

Verdijk LB, Gleeson BG, Jonkers RA, Meijer K, Savelberg HH, Dendale P, van Loon LJ. Skeletal muscle hypertrophy following resistance training is accompanied by a fiber type-specific increase in satellite cell content in elderly men. J Gerontol A Biol Sci Med Sci. 2009;64:332–9.

Xie WQ, He M, Yu DJ, Wu YX, Wang XH, Lv S, Xiao WF, Li YS. Mouse models of sarcopenia: classification and evaluation. J Cachexia Sarcopenia Muscle. 2021;12:538–54.

Xu M, Tchkonia T, Ding H, Ogrodnik M, Lubbers ER, Pirtskhalava T, White TA, Johnson KO, Stout MB, Mezera V, Giorgadze N, Jensen MD, LeBrasseur N, Kirkland JL. JAK inhibition alleviates the cellular senescence-associated secretory phenotype and frailty in old age. Proc Natl Acad Sci USA. 2015;112:E6301–10.

Xu M, Pistskhava T, Farr JN, Weigand BM, Palmer AK, Weivoda MM, Inman CL, Ogrodnik MB, Hachfeld CM, Fraser DG, Onken JL, Johson KO, Verzosa GC, Langhi LGP, Weigl M, Giorgadze N, LeBrasseur NK, Miller JD, Jurk D, Singh RJ, Allison DB, Ejima K, Hubbard GB, Ikeno Y, Cubro H, Garovic VD, Hou X, Weroha SJ, Robbins PD, Niedernhofer LJ, Khosla S, Tchkonia T, Kirkland JL. Senolytics improve physical function and increase lifespan in old age. Nature Med. 2018;24:1246–56.

Yoo A, Jang YJ, Ahn J, Jung CH, Ha TY. 2,6-Dimethoxy-1,4-benzoquinone increases skeletal muscle mass and performance by regulating AKT/mTOR signaling and mitochondrial function. Phytomedicine. 2021;91:153658.

Publisher's Note